Weak Localization in Bilayer Graphene

R. V. Gorbachev, F. V. Tikhonenko, A. S. Mayorov, D. W. Horsell, and A. K. Savchenko
School of Physics, University of Exeter, Stocker Road, Exeter, EX4 4QL, United Kingdom
(Received 30 January 2007; published 26 April 2007)

We have performed the first experimental investigation of quantum interference corrections to the conductivity of a bilayer graphene structure. A negative magnetoresistance—a signature of weak localization—is observed at different carrier densities, including the electroneutrality region. It is very different, however, from the weak localization in conventional two-dimensional systems. We show that it is controlled not only by the dephasing time, but also by different elastic processes that break the effective time-reversal symmetry and provide intervalley scattering.

DOI: 10.1103/PhysRevLett.98.176805 PACS numbers: 73.23.−b, 72.15.Rn, 73.43.Qt

The discovery that a single layer of carbon atoms (graphene [1]) can be manufactured in such a way that the carrier density is controlled by a gate voltage [1,2] became a breakthrough in creating a new, high-quality two-dimensional (2D) system. It has remarkable differences from conventional 2D systems: a linear energy spectrum and chirality of charge carriers. These initiated much interest (mainly theoretical) in exploring graphene's properties. One of them is the manifestation of well-known [3] quantum interference corrections to the conductivity.

The interference of electron waves that are scattered by disorder and form closed trajectories usually decreases the conductivity, resulting in the so-called weak localization (WL) of electrons. A perpendicular magnetic field introduces a phase difference for interfering carriers and destroys the WL, making measurements of the (positive) magnetoconductivity a sensitive tool of quantum interference. Carriers in graphene are chiral, that is, they have an additional quantum number, pseudospin, arising from the fact that their wave functions are composed of the contributions from two sublattices. If pseudospin is conserved, the backscattering of carriers is forbidden and weak antilocalization rather than WL will occur [4–6], with a positive correction to conductance and a negative magnetoconductance. Furthermore, the quantum interference in graphene will be sensitive not only to inelastic scattering of carriers, which breaks the phase of the wave function, but also to a number of elastic scattering mechanisms, especially atomically sharp and topological defects which affect the carrier chirality [5,6]. The energy spectrum "warping" of the carriers is also of major importance for WL in graphene [6]. The first experiments on WL in single-layer graphene [7–9] have indeed shown its high sensitivity to the details of scattering processes, even full suppression of the interference effect [7].

In this work we study WL in a bilayer graphene structure. It has already been understood that adding a second layer of graphene changes the system dramatically: the linear dispersion relation becomes parabolic [10,11]. In spite of this, bilayer graphene is expected to be very different from conventional 2D systems with parabolic spectrum, as well as from single-layer graphene [11–14] (as measurements of the quantum Hall effect [15,16] have already shown). The carriers remain chiral, but the Berry phase of the wave function (a measure of chirality) in a bilayer is 2π and not π as in a single layer (which means that the pseudospin turns twice as quickly in the plane than the momentum, while in a single layer it is aligned with the momentum). As a result, there will be no suppression of backscattering, and the quantum correction in a bilayer will have the sign of conventional WL [5,14]. Its magnitude, however, will still be very sensitive to different elastic processes: WL in each of the two graphene valleys can be totally suppressed by topological defects [5] and warping of the energy spectrum (the latter is expected to be stronger in a bilayer than in a single layer [14]). At the same time, intervalley scattering can partially restore WL.

Our measurements of the positive magnetoconductance of a gate-voltage controlled bilayer structure have shown the existence of WL at all studied carrier densities. The detailed analysis of the results is performed using the

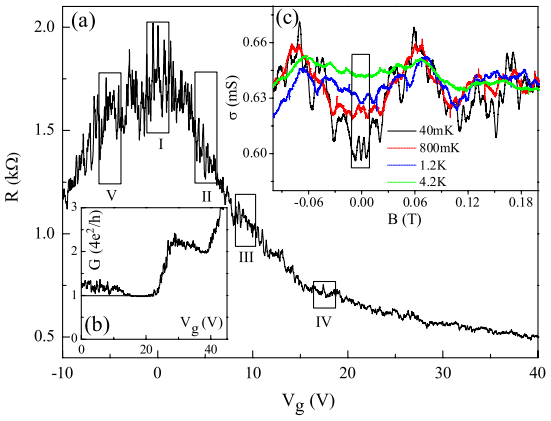

FIG. 1 (color online). (a) Dependence of the resistance of the bilayer flake on gate voltage at 40 mK. (b) Conductance as a function of V_g at $B = 14.3$ T. (c) Conductivity fluctuations as a function of magnetic field for different temperatures (region II). The rectangle defines the range of fields used for WL measurements.

 © 2007 The American Physical Society

theory [14], which has allowed us to determine three physical quantities responsible for the manifestation of WL: the phase breaking time τ_ϕ and two elastic times—the intervalley scattering time τ_i and an effective time-reversal symmetry breaking time τ_w.

The sample of rectangular shape (1.5 μm $\times$ 1.8 μm) is fabricated by the method of mechanical exfoliation of (HOPG) graphite developed in [1]. The bilayer flake is deposited on a n^+Si substrate separated by a 300 nm SiO_2 layer. Using e-beam lithography, two Au/Cr contacts were made at opposite edges of the flake to allow resistance measurements from 40 mK to 4.2 K. The carrier density up to 1.5×10^{12} cm^{-2} is varied by the gate voltage between the flake and n^+Si (in accordance with the relation $dn/dV_g = 7.3 \times 10^{10}$ cm^{-2} V^{-1} determined by the thickness of SiO_2).

Figure 1(a) shows the dependence of the sample resistance on gate voltage, with a characteristic peak in the region of electroneutrality, where the type of carrier changes from electrons (at positive V_g) to holes (at negative V_g). [A small offset in the position of the maximum of ~ -3 V, caused by unintentional doping of the flake [1], is compensated in Fig. 1(a).] The carrier mobility outside the electroneutrality region, $|V_g| \geq 5$ V, is $\sim$7000 cm^2 V^{-1} s^{-1}. The gate-voltage dependence of the resistance in strong magnetic field has shown quantum Hall plateaus that indicate that the sample is indeed bilayer graphene: the conductance quantization $\sigma_{xy} = 4Ne^2/h$, where N is an integer, occurs at Landau-level filling factors $\nu = 1/2, 3/2, \ldots$ [16]. An example of such dependence with a clear $\nu = 1/2$ plateau is given in Fig. 1(b).

In our study of WL we concentrate on a small magnetic field range indicated by the box in Fig. 1(c). Because of the mesoscopic nature of the small sample, its conductance shows reproducible fluctuations of the order of e^2/h, both as a function of V_g and B, decaying with increasing temperature, Fig. 1(a) and 1(c). The presence of the fluctuations made the magnetoconductance traces sensitive to small shifts in V_g. Therefore, we have averaged the effect of magnetic field over the range $\Delta V_g = 2$ V, which is not too large to change significantly the average resistance of the sample, but large enough to contain several $R(V_g)$ fluctuations corresponding to several "sample realizations." Five studied V_g regions are shown in Fig. 1(a).

Figure 2 illustrates our procedure of averaging. At a given temperature, we find the conductivity $\sigma(V_g)$ at several values of B field, which is changed up to ± 17 mT with a step of $\sim$1 mT. Then the average difference $\Delta\sigma(B) = \langle\sigma(B, V_g) - \sigma(0, V_g)\rangle_{\Delta V_g}$ is determined. An example of the resulting magnetoconductivity (MC) at several temperatures for regions I and II is presented in Fig. 3. To decrease further the effect of conductance fluctuations, the data in region II are averaged with those in region V which is approximately symmetric with respect to the electroneutrality point. [To find σ from the measured resistance $R(V_g)$, the resistance of the contacts, $\sim$175 Ohm, is taken into account. This value is found from the deviation of the plateau in Fig. 1(b) from the expected quantized value of $4e^2/h$.]

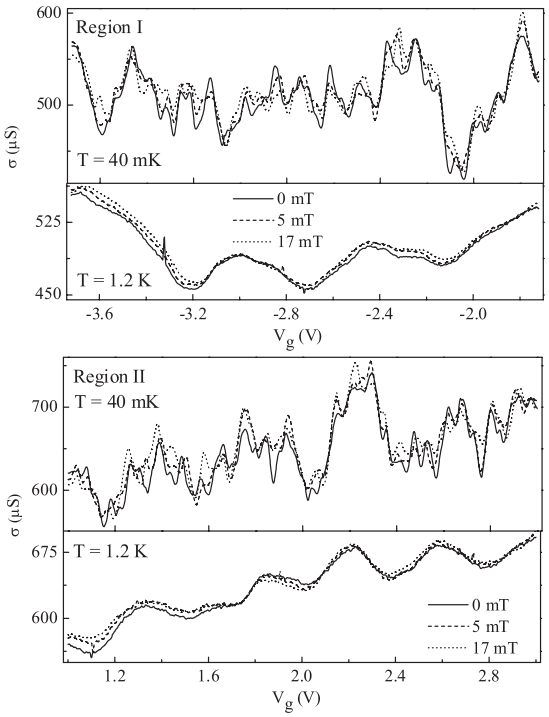

FIG. 2. Evolution of conductance fluctuations with small magnetic fields applied, for regions I and II.

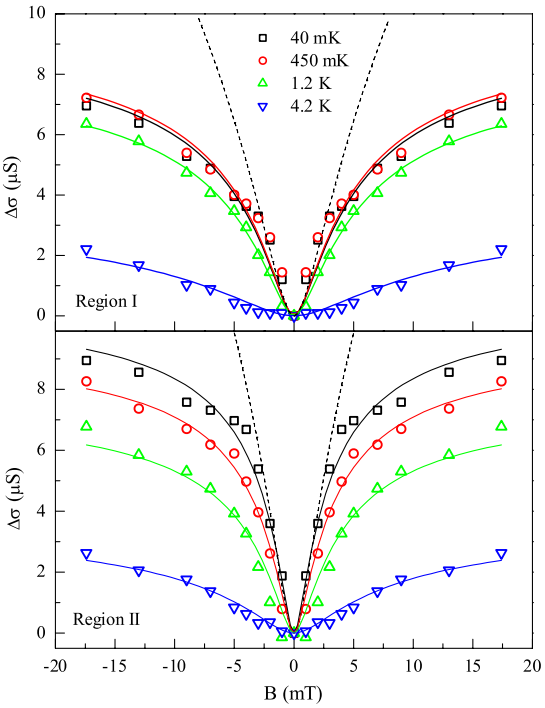

FIG. 3 (color online). Averaged magnetoconductivity for regions I and II. Dashed curves are the fits using only the first term in Eq. (1), and solid lines are the fits with the first two terms.

To analyze the results we use the following expression for the MC due to WL in bilayer graphene [14]:

$$\Delta\sigma(B) = \frac{e^2}{\pi h}\left[F\left(\frac{B}{B_\phi}\right) - F\left(\frac{B}{B_\phi + 2B_i}\right) + 2F\left(\frac{B}{B_\phi + B_*}\right)\right],$$
$$F(z) = \ln z + \psi\left(\frac{1}{2} + \frac{1}{z}\right), \qquad B_{\phi,i,*} = \frac{\hbar}{4De}\tau^{-1}_{\phi,i,*}. \qquad (1)$$

Here $\psi(x)$ is the digamma function, τ_ϕ is the phase breaking time, τ_i is the intervalley scattering time, and $(\tau_*)^{-1} = (\tau_i)^{-1} + (\tau_w)^{-1}$, where τ_w is the intravalley warping time combined with the time of chirality breaking [5]. Equation (1) contains three terms, and its main difference from the single-layer result [6] is in the positive sign of the third term. It is seen that in the case of τ_i, $\tau_* \to \infty$, i.e., in the absence of the corresponding elastic scattering, the MC is reduced to the third term and becomes the conventional expression for WL in a 2D system with two valleys, with a positive MC. On the contrary, strong warping scattering ($\tau_w \to 0$) without intervalley scattering ($\tau_i \to \infty$) suppresses the third term while the first two cancel each other—the result is zero MC (complete suppression of WL). However, introducing some intervalley scattering ($\tau_i \sim \tau_\phi$) will make the second term smaller than the first, so that there will be no full cancellation and the first term will dominate in small fields. The result will be a conventional, positive MC, although with a suppression factor of $1/2$. We will now see that it is exactly this situation that describes the experimental results.

Figure 3 shows that the MC in very small fields can be indeed satisfactorily approximated by the first term in Eq. (1), but with increasing B this approximation strongly deviates towards larger values. Inclusion of the second (negative) term allows one to get good agreement with experiment over the whole field range and obtain values of the temperature-dependent dephasing time τ_ϕ and temperature-independent intervalley time τ_i. [Somewhat better agreement can be achieved by including the third term of Eq. (1), from which the value of the warping time can be estimated—see below.]

We start the discussion of the results by noting that the conductivity of our sample is always larger than e^2/h, Fig. 1, and therefore the pertubation theory of WL is applicable in the whole range of V_g. Analysis of the data with the first two terms in Eq. (1) (assuming strong warping, $\tau_w \to 0$) gives the value of the coherence length $L_\phi = (D\tau_\phi)^{1/2}$ and the phase breaking time τ_ϕ, Fig. 4(a). The diffusion coefficient is found from the relation $D = \sigma\pi\hbar^2/2m^*e^2$, where σ is the average conductivity in each region and $m^* = 0.033\ m_0$ is the effective mass of carriers in graphene bilayers [11].

The manifestation of WL in region I deserves special consideration. It is reasonable to assume that when the average carrier density is close to zero, the presence of disorder splits the system into electron-hole puddles [17] separated by p-n junctions [12,18]. [A rough estimation of the carrier density in the puddles, n, $p \le 3 \times 10^{11}$ cm^{-2}, can be obtained from the range $|V_g| \le 4$ V where, ignoring the fluctuations, the dependence $R(V_g)$ in Fig. 1 flattens out.] The fact that WL in region I is not suppressed means that breaking down the system into puddles does not prevent interference of charge carriers on a scale larger than the puddle size. A possible reason for this is that the p-n junctions separating the puddles are highly transparent (at some angles of incidence) for chiral carriers [12,18], and therefore carrier transitions between the puddles can occur in a coherent way.

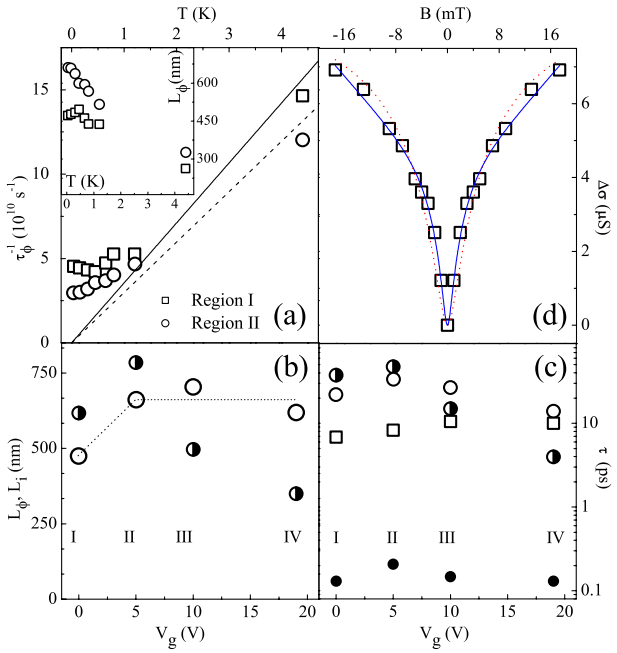

FIG. 4 (color online). (a) Temperature dependence of the dephasing rate for regions I and II fitted with linear dependence. Inset: coherence length as a function of temperature for the two V_g regions. (b) Coherence length at 40 mK (open circles) and intervalley scattering length (half-filled circles) for different V_g regions. (Dotted line is a guide to the eye.) (c) Dephasing time at 40 mK (open circles) and 4.2 K (squares) in comparison with the intervalley time (half-filled circles) and momentum relaxation time (filled circles). (d) Comparison of the fits with two terms (dotted line) and three terms (solid line) in Eq. (1) for the 40 mK curve in region I, Fig. 3.

Figure 4(a) compares $L_\phi(T)$ and $\tau_\phi(T)$ in regions I and II. It is seen that the coherence length increases with decreasing T but approaches a finite value at $T \to 0$, which is also seen as an offset in $\tau_\phi^{-1}(T)$. [Our preliminary analysis of the $\sigma(B)$ fluctuations as universal conductance fluctuations has given similar magnitude and behavior of $L_\phi(T)$.] There is a natural explanation that the increase of L_ϕ at low temperatures is limited by the size of the sample, $L = 1.5\ \mu$m. The somewhat smaller saturation value of L_ϕ in region I can be treated as an indication of the formation of puddles in the electroneutrality region. Charge carriers inside a puddle have to scatter several times from its boundary before finding an optimal angle

to penetrate the p-n junction. This results in an effective decrease of their coherence length.

The increase of the dephasing rate with temperature in all regions agrees with the prediction of the theory of electron-electron interaction in the diffusive regime [19], where $k_B T\tau_p/\hbar < 1$. This regime is indeed realized in our sample where the parameter $k_B T\tau_p/\hbar$ varies from 0.001 to 0.1. We have approximated the experimental temperature dependence of the dephasing rate at $T > 1$ K as $\tau_\varphi^{-1} = \beta k_B T \ln g/(\hbar g)$, where $g = \sigma h/e^2$ is the dimensionless conductivity. The empirical coefficient β is found to be close to unity: $\sim$1.2 in all regions, Fig. 4(a).

Figure 4(b) shows the low-T saturation value of L_ϕ. It is close to half the length of the sample in all regions apart from region I where it gets smaller, which we tentatively ascribe to the formation of the puddles. Also shown is the temperature-independent intervalley diffusion length $L_i = (D\tau_i)^{1/2}$. This can be interpreted as a characteristic distance between defects that are able to change significantly the momentum of charge carriers. By comparing this distance with the size of the sample, one can estimate the number of such defects: $\sim$10.

Figure 4(c) compares, in several V_g regions, the phase breaking time τ_ϕ with the intervalley scattering time τ_i and momentum relaxation time τ_p. One can see that τ_ϕ and τ_i are of the same order of magnitude and much larger than $\tau_p \sim 0.15$ ps. An estimation of the warping time can be obtained by taking into consideration the third term in Eq. (1). It has less effect on the description of the MC and does not change much the values of τ_ϕ and τ_i found earlier. Figure 4(d) illustrates the degree of improvement of the fit with inclusion of the third term. By considering its contribution, we obtain the following estimation of the warping time in the studied V_g regions: $\tau_* \sim \tau_w \lesssim 0.5$ ps, which is close to the estimation [14] of the warping time in bilayer graphene at densities $\sim 10^{12}$ cm^{-2}: $\tau_w \sim \tau_p$. The small value of the obtained τ_w is consistent with the smallness of the third term and is a clear signature of the importance of the warping in the studied system.

It is interesting to compare our values of τ_i with that recently obtained from the analysis of WL in single-layer graphene [8]. The sample in [8] was fabricated by a different method (thermal decomposition of SiC) and studied at a larger electron density, $n = 3.4 \times 10^{12}$ cm^{-2}. The dephasing time (for similar temperatures) and the momentum relaxation time are close in both cases. The intervalley scattering time, however, in our experiment is 10–30 times larger than in [8]. As the intervalley scattering is controlled by atomically sharp impurities, the difference in the concentration of these impurities can be due to the difference in the fabrication techniques. Alternatively, the difference in τ_i can be caused by the intrinsic difference between single-layer and bilayer: scattering by sharp defects can be of less importance in a more robust system with two layers.

In conclusion, we have performed an experimental investigation of the magnetoresistance caused by weak localization in bilayer graphene controlled by gate voltage. Several ranges of V_g, including the electroneutrality region, have been studied. First, we have found that WL is not suppressed in all regions. Second, we have found good agreement of our results with the prediction of the theory of WL in bilayer graphene [14], and we have determined the values of the characteristic times which make the manifestation of WL in bilayer graphene different from that in conventional 2D systems.

We are grateful to A. Geim, K. Novoselov, and D. Jiang for sharing their knowledge of the fabrication of graphene flakes by mechanical exfoliation. We are indebted to V. I. Fal'ko, E. McCann, and K. Kechedzhi for discussing their results prior to publication. We also acknowledge useful discussions with V. V. Cheianov, P. Kim, F. Guinea, and A. Castro Neto concerning the physics of graphene-based structures.

[1] K. S. Novoselov *et al.*, Science **306**, 666 (2004).
[2] Y. Zhang *et al.*, Phys. Rev. Lett. **94**, 176803 (2005).
[3] B. L. Altshuler *et al.*, Phys. Rev. B **22**, 5142 (1980); G. Bergman, Phys. Rep. **107**, 1 (1984).
[4] H. Suzuura and T. Ando, Phys. Rev. Lett. **89**, 266603 (2002); D. V. Khveshchenko, *ibid.* **97**, 036802 (2006); I. L. Aleiner and K. B. Efetov, *ibid.* **97**, 236801 (2006); P. M. Ostrovsy, I. V. Gornyi, and A. D. Mirlin, Phys. Rev. B **74**, 235443 (2006).
[5] A. F. Morpurgo and F. Guinea, Phys. Rev. Lett. **97**, 196804 (2006).
[6] E. McCann *et al.*, Phys. Rev. Lett. **97**, 146805 (2006).
[7] S. V. Morozov *et al.*, Phys. Rev. Lett. **97**, 016801 (2006).
[8] X. Wu *et al.*, Phys. Rev. Lett. **98**, 136801 (2007).
[9] H. B. Heersche *et al.*, Nature (London) **446**, 56 (2007).
[10] B. Partoens and F. M. Peeters, Phys. Rev. B **74**, 075404 (2006); F. Guinea, A. H. Castro Neto, and N. M. R. Peres, *ibid.* **73**, 245426 (2006).
[11] E. McCann and V. I. Fal'ko, Phys. Rev. Lett. **96**, 086805 (2006); M. Koshino and T. Ando, Phys. Rev. B **73**, 245403 (2006); T. Ohta *et al.*, Science **313**, 951 (2006).
[12] M. I. Katsnelson, K. S. Novoselov, and A. K. Geim, Nature Phys. **2**, 620 (2006).
[13] J. Nilsson *et al.*, Phys. Rev. B **73**, 214418 (2006); M. Katsnelson, Eur. Phys. J. B **52**, 151 (2006); I. Snyman and C. W. J. Beenaker, Phys. Rev. B **75**, 045322 (2007).
[14] K. Kechedzhi *et al.*, Phys. Rev. Lett., this issue, **98**, 176806 (2007).
[15] K. S. Novoselov *et al.*, Nature (London) **438**, 197 (2005); Y. Zhang *et al.*, *ibid.* **438**, 201 (2005).
[16] K. S. Novoselov *et al.*, Nature Phys. **2**, 177 (2006).
[17] E. H. Hwang, S. Adam, and S. Das Sarma, cond-mat/0610157 [Phys. Rev. Lett. (to be published)].
[18] V. V. Cheianov and V. I. Fal'ko, Phys. Rev. B **74**, 041403 (2006).
[19] B. I. Altshuler, A. G. Aronov, and D. E. Khmelnitsky, J. Phys. C **15**, 7367 (1982).